

SN 1988Z: Spectro-photometric catalogue and energy estimates[★]

Itziar Aretxaga^{1,2†}, S. Benetti³, R. J. Terlevich^{4‡}, A.C. Fabian⁴,
E. Cappellaro⁵, M. Turatto⁵ and M. Della Valle^{6,7}

¹ *Max-Planck-Institut für Astrophysik, Karl Schwarzschildstr. 1, Postfach 1523, 85740 Garching, Germany*

² *Instituto Nacional de Astrofísica, Óptica y Electrónica, Apto. Postal 51 y 216, Puebla, Mexico*

³ *Telescopio Nazionale Galileo, Apto. Correos 565, E-38700 Santa Cruz de La Palma, Canary Islands, Spain*

⁴ *Institute of Astronomy, Madingley Road, Cambridge CB3 0HA, U.K.*

⁵ *Oss. Astronomico di Padova, vicolo dell'Osservatorio 5, I-35122, Italy*

⁶ *Dipar. di Astronomia, Univ. di Padova, vicolo dell'Osservatorio 5, I-35122, Italy*

⁷ *European Southern Observatory, Alonso de Cordova 3107, Vitacura, Casilla 19001, Santiago 19, Chile.*

ABSTRACT

We present a spectro-photometric catalogue of the evolution of supernova 1988Z which combines new and published observations in the radio, optical and X-ray bands, with the aim of offering a comprehensive view of the evolution of this object and deriving the total energy radiated since discovery. The major contribution to the total radiated energy comes at optical to X-ray frequencies, with a total emission of at least 2×10^{51} erg (for $H_0 = 50 \text{ km s}^{-1} \text{ Mpc}^{-1}$) in 8.5 years. A model-dependent extrapolation of this value indicates that the total radiated energy may be as high as 10^{52} erg. The high value of the radiated energy supports a scenario in which most of the kinetic energy of the ejecta is thermalized and radiated in a short interaction with a dense circumstellar medium of nearly constant density. In this sense, 1988Z is not a supernova but a young and compact supernova remnant.

Key words: supernovae: individual: SN 1988Z – supernova remnants

1. INTRODUCTION

The explosion of massive stars, thought to take place as the result of pair formation, collapse of a Fe core or neutronization of an ONeMg degenerate core, leads to supernovae (SN) that show H signatures in their spectra and thus are classified as type II. These objects display a wide range of observational properties which justifies the existence of the two photometric sub-classes, II-P and II-L (Barbon, Ciatti & Rosino 1979), and the recent introduction of the peculiar spectroscopic sub-group IIn (Schlegel 1990).

The spectra of SN IIn are characterized by the presence of prominent narrow emission lines sitting on top of broad components of $\text{FWHM} \approx 15000 \text{ km/s}$ at maximum light which look very similar to those of Seyfert 1 nuclei and QSOs (Filippenko 1989). They don't show the characteristic broad P-Cygni signatures of standard SN, although narrow P-Cygni profiles are detected in some cases at high spectral

resolution (SN 1997ab, Salamanca et al. 1998; SN 1995G, ESO data archive; SN 1997eg, Tenorio-Tagle G., priv. communication). SN IIn are normally associated with regions of recent star formation. Despite these general characteristics, SN IIn as a group exhibit some heterogeneity (see Filippenko 1997, Turatto et al. 1999).

SN 1988Z, one of the most extensively observed SN of this class, was discovered in 1988 December 12 in the galaxy M+03-28-022 (Zw 095-049) (Cappellaro & Turatto 1988, Pollas 1988a). Earlier observations in late spring 1988 show no evidence of the event (Turatto et al. 1993a). This is an exceptionally bright and peculiar SN in its spectro-photometric properties:

- It is characterized by an extremely slow decay of luminosity after maximum light, which makes it at day 600 approximately 5 mag brighter in the V-band than standard SN II-P or SN II-L (Stathakis & Sadler 1991).
- It has a strong $H\alpha$ emission, with peak luminosities of about $4 \times 10^{41} \text{ erg s}^{-1}$ (for $H_0 = 50 \text{ km s}^{-1} \text{ Mpc}^{-1}$) at day 200 (Turatto et al. 1993a). This prodigious luminosity is 5 orders of magnitude larger than that of SN 1987A.
- Very high-ionization coronal lines (e.g. $[\text{Fe X}]\lambda 6375 \text{ \AA}$,

[★] Based on observation carried out at ESO La Silla

[†] Present address: INAOE, Puebla, Mexico

[‡] Visiting Professor at INAOE, Puebla, Mexico

[Fe XI] λ 7889-7892 Å) are identified in the optical spectra, at least until day 492 (Turatto et al. 1993a).

- At 2 to 20cm it is one of the most powerful radio-SN in the sky, with peak-luminosities up to 3000 times that of remnants like Cas A (Van Dyk et al. 1993).

- Even 6 yr after maximum the SN shows an X-ray emission of more than 10^{41} erg s $^{-1}$ (Fabian & Terlevich 1996).

The summary of these points is that this is one of the most energetic radiative events known to be generated in a single stellar object.

These radiative properties have been interpreted in the light of quick re-processing of the mechanical energy of a SN explosion by a dense circumstellar medium (CSM) (Chugai 1991, Terlevich et al. 1992, Terlevich 1994, Chugai & Danziger 1994, Plewa 1995). As explained in the appendix, radiative cooling is expected to become important well before the thermalization of the ejecta is complete. As a result, the shocked material undergoes a rapid condensation behind both the leading and reverse shocks. These high-density thin shells, the freely expanding ejecta and the still unperturbed interstellar gas are all ionized by the radiation produced in the shocks, and are responsible for the complex emission line structure observed in these objects.

In the case of SN 1988Z, a direct measurement of the CSM electron density was possible. The value determined from the [OIII] λ 4363 Å to [OIII] λ 5007 Å forbidden line ratio in the early stages of the evolution is between 4×10^6 and 1.6×10^7 cm $^{-3}$ (Stathakis & Sadler 1991). This high density points towards SN 1988Z in particular, and SN IIn in general, being young compact SN remnants (cSNR).

In this paper we present new optical and X-ray spectrophotometric observations of the late evolution (4.3 to 8.5 yr) of this object, which combined with already published information on its early evolution, aims at deriving the total energy radiated since discovery, and shedding new light into the mechanism that generates such a long-lasting bright event.

2. DATA SET

2.1. Optical observations

The new optical observations that we present in this paper span a period of about 4 years, starting 4.3 years after discovery.

B, *V* and *R*-band photometry of SN 1988Z was obtained at the European Southern Observatory (ESO) in La Silla on six nights between 1993 March 27 and 1997 February 10 using the 3.6m telescope in combination with the ESO Faint Object Spectrograph and Camera (EFOSC1) and the 3.5m New Technology Telescope (NTT) with the ESO Multi Mode Instrument (EMMI) or the Superb Seeing Imager (SUSI).

When the nights were photometric the magnitudes were calibrated using a number of Landolt's (1992) standard stars. In non-photometric nights the SN magnitudes were derived using the local sequence defined in Turatto et al. (1993a). The SN magnitudes were measured by fitting a

point spread function with the ROMAFOT package of MIDAS. This technique allows a good subtraction of the background and gives reliable results even for faint objects (see Turatto et al. 1993b). The journal of observations together with the resulting magnitudes and an estimate of the internal errors are reported in table 1, where age refers to the time elapsed since the SN discovery, 1988 December 12 (JD 24447508).

The journal of the spectroscopic observations is given in table 2, where for each spectrum column 1 gives the date of acquisition, column 2 the age, column 3 the instrumentation used, column 4 the exposure time, column 5 the wavelength range and column 6 the resolution derived from the average FWHM of the night-sky lines. In two epochs we obtained spectra during two consecutive nights. In these cases we co-added the spectra to reach higher signal-to-noise ratios and included the cumulative exposure times in column 4. The spectra were wavelength calibrated with He- λ Ar arcs and flux calibrated using standard stars from the list of Hamuy et al. (1994). The absolute flux calibration of the spectra was verified against the broad-band photometry and the agreement was generally fair.

Figure 1 shows as an example of its late stages in evolution, the spectrum of SN 1988Z on 1996 February 14. The earlier evolution of the spectrum can be seen in Stathakis & Sadler (1991), Filippenko (1991) and Turatto et al. (1993a).

2.2. X-ray data

SN 1988Z has been observed three times with the *Röntgensatellit* (ROSAT) High Resolution Imager (HRI), in 1995 (detection reported in Fabian & Terlevich 1996), 1996 and 1997. Table 3 summarizes these observations.

Only the first and last observations provide a good detection of the object; the middle one was too short. The count rate declined from 1.1×10^{-3} to 3.7×10^{-4} s $^{-1}$ between 1995 May and 1997 May. Using Poisson statistics on the numbers of counts detected, we find that the probability that the average count rate was equal to or higher than that seen in 1995, and equal to or lower than that seen in 1997 is less than 0.2 per cent, adopting the weighted mean of both observations at both times. This indicates that the decrease is statistically significant.

The 0.2–2 keV fluxes, corrected for absorption in our Galaxy $N_H = 2.5 \times 10^{20}$ cm $^{-2}$ (Burstein & Heiles 1982), are given in table 3, assuming a 1 keV bremsstrahlung spectrum. The 0.2–2 keV luminosity therefore dropped from $(8 \pm 3.2) \times 10^{40}$ erg s $^{-1}$ in 1995 to $(3 \pm 1.6) \times 10^{40}$ erg s $^{-1}$ in 1997.

These are probably underestimates of the X-ray luminosity. The hydrogen column density can be much higher than that assumed if the pre-ionized CSM is only partially ionized. Using the photoionization code CLOUDY 90 (Ferland 1997) and a description of the evolution of the leading shock of SN 1988Z based on the model by Terlevich (1994) (see appendix) we estimate that if the mass of the CSM still to be swept is of the order of $1M_\odot$, then the column density would be of the order of 10^{22} cm $^{-2}$ at $t = 12t_{sg}$, where t_{sg} refers to the time of the radiative onset of the remnant (eq. A3), around 250 days from core collapse for this object. For a column density of 10^{22} cm $^{-2}$ the previous estimates of the X-ray luminosity should be increased by a factor of eight if we assume a 1 keV temperature. The bolometric lu-

Table 1. Broad-band photometry

date	age days	B mag	V mag	R mag	instrument
1993 Mar 27	1565	22.23 ± 0.26	22.08 ± 0.25	20.79 ± 0.20	NTT + EMMI
1994 Jan 14	1856			21.36 ± 0.20	3.6m + EFOSC1
1994 Dec 30	2209			21.71 ± 0.20	NTT + EMMI
1995 Jan 10	2220		22.73 ± 0.20	21.70 ± 0.15	NTT + SUSI
1996 Feb 14	2620			21.87 ± 0.20	3.6m + EFOSC1
1997 Feb 10	2982			22.04 ± 0.20	3.6m + EFOSC1

Table 2. Journal of spectroscopic observations

date	age days	instrument	exp. min	range Å	resol. Å
1993 Mar 27	1565	NTT + EMMI	105	3750-9700	13
1994 Jan 13-14	1859	3.6m + EFOSC1	115	3700-6900	16
1994 Dec 30	2209	NTT + EMMI	90	3700-8900	8
1996 Feb 14	2620	3.6m + EFOSC1	120	3750-6950	16
1997 Feb 9-10	2982	3.6m + EFOSC1	240	3730-6900	16

minosities for the assumed spectrum are 1.6 times greater. We should emphasize that the absorption history is very dependent in the total CSM mass. For larger CSM masses the recombination occurs earlier in the evolution and thus the soft X-ray correction is larger.

ROSAT observations of SN 1986J, another SN IIn, also show a high column density of 10^{22}cm^{-2} and a prominent X-ray luminosity $2 - 3 \times 10^{40} \text{erg s}^{-1}$ about 9 years after the SN event (Bregman & Pildis 1992).

2.3. Catalogue of radio, optical and X-ray photometry

A compilation of photometric data gathered from the literature, combined with the new spectro-photometric observations introduced in sections 2.1 and 2.2 is presented in table 4. Column 1 gives the age since discovery. Columns 2 to 10 give the flux and apparent magnitude of the object in the 0.2 to 2 keV band from ROSAT; *B*, *V*, *R*-band photometry and $\text{H}\alpha$ flux from spectroscopy obtained with ground-based optical telescopes; and 2 to 20 cm fluxes from VLA. All fluxes are corrected for Galactic extinction using Seaton’s law (1979). Column 11 gives the reference from which the data was extracted, where SS91 refers to Stathakis & Sadler (1991), T93 to Turatto et al. (1993a), FT96 to Fabian & Terlevich (1996) and IAUC to the IAU circulars numbers 4691, 4696, 4742 and 4761. (Cappellaro & Turatto 1988; Pollas 1988a, 1988b, 1989; Gaskell & Koratkar 1989)

Figure 2 shows a combined representation of the light curves of SN 1988Z at different frequencies. In the area occupied by the optical and X-ray data, solid crosses correspond to $\text{H}\alpha$, solid squares to *R*-band, solid triangles to *V*-band, open triangles to *B*-band and the solid hexagons to the ROSAT 0.2 to 2 keV band.

The thin solid line that passes through the broad-band optical and X-ray points describes a $t^{-11/7}$ law. This is a semi-analytic approximation of the bolometric emission produced by a cSNR when it evolves in a dense CSM of homo-

geneus density (eq. A7) having the canonical value of density of the CSM 10^7cm^{-3} , and being scaled to match the *V*-band luminosity of SN 1988Z. The overall decline is remarkably well followed by this law, even at time-scales for which the assumptions of the semi-analytic approximations are no longer valid ($t \gtrsim 250$ days). The dashed line that passes through the $\text{H}\alpha$ points represents the $\text{H}\alpha$ luminosity predicted by the same models (Terlevich 1994), with no intrinsic scaling. Although the models predict the peak of $\text{H}\alpha$ luminosity correctly at day ~ 200 , in the late evolution of the SN they fail to reproduce the more pronounced decay by about an order of magnitude.

The lines that pass through the radio points are the models of an external thermal-absorbing gas combined with an internal thermal-absorbing/non-thermal-emitting gas fitted by Van Dyk et al. (1993) to their VLA observations.

Since $\text{H}\alpha$, at the recession velocity of SN 1988Z $v_r = 6670 \text{km s}^{-1}$ (Barbon, Cappellaro & Turatto 1989), is fully included in the *R* pass-band we have estimated a $\text{H}\alpha$ line-free *R*-band magnitude subtracting an interpolated $\text{H}\alpha$ flux from table 4 as

$$R_{\text{cont}} = -2.5 \log \left(10^{-R/2.5} - \frac{0.80 f(\text{H}\alpha)}{f_R^0} \right), \quad (1)$$

where f_R^0 is the photometric zero of *R*-band in the same units as $f(\text{H}\alpha)$, and the 0.80 factor represents the transmission value of the redshifted $\text{H}\alpha$ line relative to the peak transmission value of the *R*-band filter used in the observations (see figure 3). The corrected *R*-band magnitudes (R_{cont}) are represented with empty squares in figure 2.

3. SPECTRAL LINE ANALYSIS

Figure 4 and 5 show the evolution of the $\text{H}\alpha$ and $\text{H}\beta$ profiles as a function of age, from days 155 to 2981.

Following the analysis performed by Turatto et al. (1993a), we report in table 5 the main emission line parameters as measured with the ALICE package in MIDAS.

Table 3. ROSAT HRI data for SN 1988Z. The 5th column tabulates the probability that the counts seen are a random fluctuation in the background. The flux in the 6th column has been corrected for Galactic absorption.

date	age days	count rate 10^{-4} s^{-1}	exp. s	random chance	flux (0.2–2 keV) $\times 10^{-14} \text{ erg s}^{-1} \text{ cm}^{-2}$
1995 May 16–25	2355	11 ± 4	12287	2×10^{-5}	4 ± 1.6
1996 Dec 14	2924	5 ± 4	6739	0.1	2 ± 1.6
1997 May 13–24	3085	3.7 ± 2	34300	0.02	1.5 ± 0.8

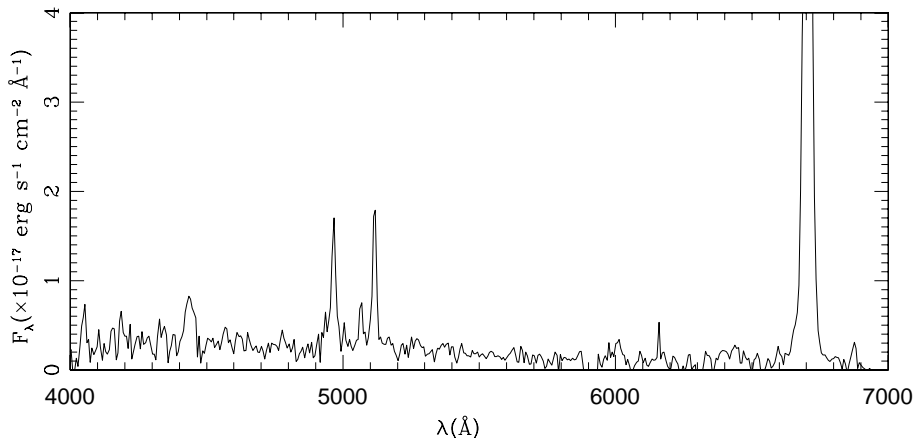


Figure 1. Spectrum of SN 1988Z on 1996 February 14.

This package allows multiple gaussian fitting of complex line profiles. The coding for broad, intermediate and narrow components follows that adopted in Turatto et al. (1993a). These were the components identified in the early evolution of SN 1988Z which we are following at later epochs. The analysis presented here is thus fully complementary with the results presented in that report. Figure 6 shows the decomposition performed in the $H\alpha$ line of the spectrum taken on 1996 February 14 as an example. In table 5 a colon indicates that the value is uncertain.

The decrease of the width of the broad component of $H\alpha$, shown in figure 7 with filled squares, is monotonical. The behaviour can be described by a power-law, which is similar to the time evolution of the velocity of the outer shock generated by a supernova remnant which evolves in a high-density medium, $t^{-5/7}$ (eq. A5), and which is plotted as a dashed-line. The law has been scaled to the velocity width of the line $\sim 4000 \text{ km/s}$ at day 1000. By comparison, the width of the intermediate component of $H\alpha$ (plotted with empty squares) decreases in a much slower way.

Figures 8 and 9 show the observed trend of the Balmer decrement and the $[O \text{ III}]\lambda 5007 \text{ \AA}$ luminosity with time. Both show an initial increase followed by a sharp down turn and a slower decay. Also shown in Figure 8 are the predictions of the simple model of cSNR evolution. In qualitative terms the observations follow the trend prescribed by the simple model. The discrepancies, though, strongly suggests that there are fundamental aspects that are not considered

by this model. These discrepancies together with the evolution of the line profiles an multifrequency light curve, will be the basis for the construction of more detailed numerical models which will include the role played by the density profile of the ejecta and the time dependent aspects of the CSM evolution.

4. PHOTOMETRIC ANALYSIS

4.1. Spectral Energy Distribution

In figure 2 we observe that the light evolution in different bands peaks at different times: first in the optical, before discovery; then in $H\alpha$ (i.e. in the ionizing continuum), between 100 and 500 days; and lastly at radio-frequencies between 400 and 2000 days. The spectral energy distribution (SED) thus changes with time.

In order to include the ionizing radiation, which is absorbed by the cool material, we estimate its value from the flux of a prominent recombination line. $H\alpha$ is particularly useful, since several percent of the ionizing energy is re-radiated through this line. Assuming case B recombination at 10000 K, which is the average temperature of the gas that emits broad lines in the hydrodynamical models of cSNR (Terlevich et al. 1992), we can convert the $H\alpha$ flux to ionizing flux. The ionizing flux f_{ion} is related to the flux of ionizing photons $q(H^0)$ by

Table 4. Photometric evolution from X-ray to radio

Age day	$f_{0.2-2\text{ keV}}$ erg cm ⁻² s ⁻¹	B mag	V mag	R mag	$f_{\text{H}\alpha}$ erg cm ⁻² s ⁻¹	$f_{2\text{ cm}}$ mJy	$f_{3.6\text{ cm}}$ mJy	$f_{6\text{ cm}}$ mJy	$f_{20\text{ cm}}$ mJy	reference
0		16.54								T93
2		16.59	16.23	15.93						T93
4		16.59		15.98						T93+IAUC
23		16.71	16.46	16.04						SS91
24		16.69								T93
34					1478×10 ⁻¹⁶					SS91
50		16.84								T93
53		17.04	16.79							T93
57			16.68	16.35						IAUC
59			16.82	16.37						IAUC
62					1669×10 ⁻¹⁶					SS91
85		17.44								T93
87		18.65	17.53							T93
91			17.59							IAUC
114		17.93	17.87							T93
115			17.74	17.47	1449×10 ⁻¹⁶					T93
117			17.91							T93
137		18.03	17.74	17.53						T93
199					1630×10 ⁻¹⁶					SS91
282			19.02	17.80						T93
392							0.67			vD93
407			19.34	18.05						T93
441		19.47	19.12	18.10						T93
446							0.77			vD93
451			19.19							T93
464					1656×10 ⁻¹⁶					SS91
474				18.09						T93
492					1947×10 ⁻¹⁶					T93
552							1.21			vD91
557			19.54	18.38						SS91
596							1.26	2.10		vD93
653							1.38		1.15	vD93
684					1019×10 ⁻¹⁶					T93
717					936×10 ⁻¹⁶					T93
731		20.78	20.16							T93
736			20.25							T93
738					730×10 ⁻¹⁶					T93
743		20.79	20.09	18.88						T93
751							1.78	2.09	1.43	vD93
758					793×10 ⁻¹⁶					T93
759				18.82						T93
798		20.89	20.24	18.94	814×10 ⁻¹⁶					T93
800				19.11						T93
845		21.29	20.61	19.08						T93
930						0.47	1.90	1.68	1.31	vD93
1028							1.85	1.48	0.59	vD93
1086			20.82	19.53						T93
1095			20.59	19.48						T93
1148		21.47	20.89	19.76						T93
1149					338×10 ⁻¹⁶					T93
1160						1.05	1.67	1.50	1.17	vD93
1420						0.91	1.57	1.22	0.91	vD93
1487						1.45	1.72	1.04	0.78	vD93
1565		22.02	21.92	20.67	124×10 ⁻¹⁶					this paper
1856				21.24	84.7×10 ⁻¹⁶					this paper
2209				21.59	56.0×10 ⁻¹⁶					this paper
2220			22.57	21.58						this paper
2355	4×10 ^{-14a}									FT96
2620				21.87	37.6×10 ⁻¹⁶					this paper
2924	2×10 ⁻¹⁴									this paper
2982				22.04	22.2×10 ⁻¹⁶					this paper
3085	1.5×10 ⁻¹⁴									this paper

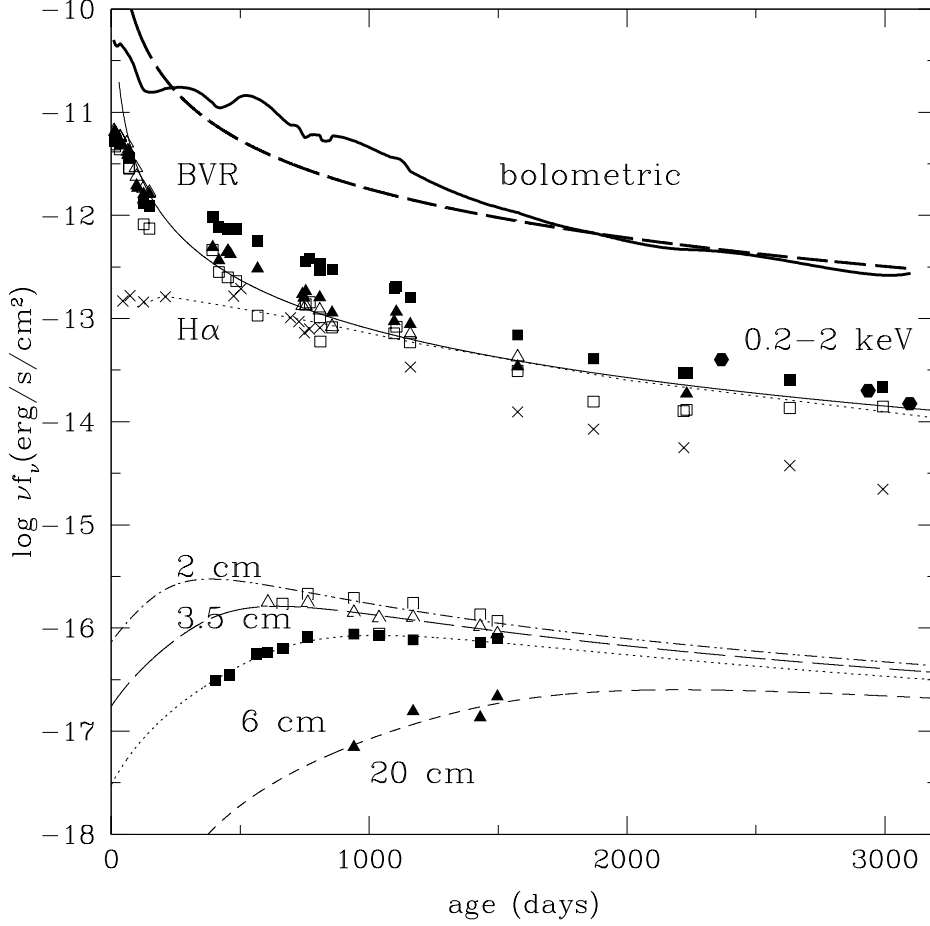


Figure 2. Evolution of the νf_ν light curve in radio to X-ray bands. In the upper part of the panel open triangles correspond to B -band, solid triangles to V -band, solid squares to R -band, empty squares to R_{cont} band, solid hexagons to the ROSAT 0.2 to 2 keV band and crosses to $H\alpha$. The thin solid and dashed lines are models for the bolometric light (scaled to the values of the optical data) and $H\alpha$ evolution of a cSNR. In the lower part of the panel, the VLA radio data at 2, 5.5, 6 and 20 cm is represented with empty squares, empty triangles, solid squares and empty triangles. The line fittings correspond to the models of Van Dyk et al. (1993). The thick solid line on the top of the panel shows the strong lower limit estimate while the thick dashed line represents our best estimate of the bolometric light curve of SN 1988Z (see section 4.2).

Table 5. Spectral line decomposition of the late spectra of SN 1988Z

age days		$H\alpha$		$H\beta$		HeI–NaID
		broad	interm.	interm.	narrow	
1565	FWHM (\AA)	48.6	25.1			75:
	flux ($\times 10^{-16} \text{ erg s}^{-1} \text{ cm}^{-2}$)	26	98			6:
1859	FWHM (\AA)	40.7	28.3	60.9	16.3	25.3
	flux ($\times 10^{-16} \text{ erg s}^{-1} \text{ cm}^{-2}$)	8	67	2.7	3.0	2.2
2209	FWHM (\AA)	49.2	27.3		18.6	47:
	flux ($\times 10^{-16} \text{ erg s}^{-1} \text{ cm}^{-2}$)	5	47		2	1.4:
2620	FWHM (\AA)	45.1	28.6	61.1	16	21:
	flux ($\times 10^{-16} \text{ erg s}^{-1} \text{ cm}^{-2}$)	9.6	24	1.7	1.9	0.4:
2981	FWHM (\AA)	53.9	25.3	45.7	16.7	51.2
	flux ($\times 10^{-16} \text{ erg s}^{-1} \text{ cm}^{-2}$)	6.9	12.9	1.2	1.3	1.0

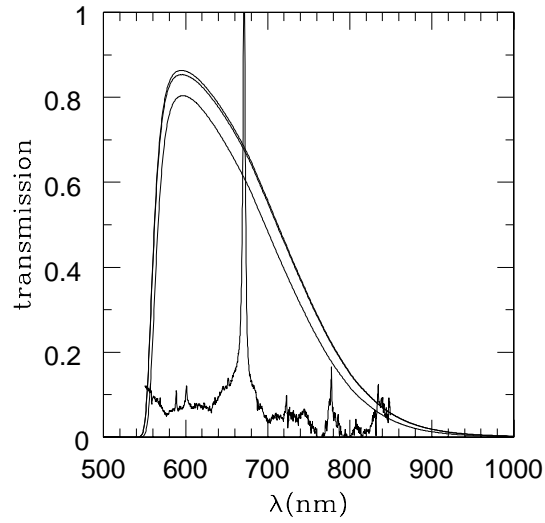


Figure 3. Transmission values of the three *R*-band filters used in the observations (ESO#554, ESO#608, ESO#642). Also plotted is the H α spectral region of SN 1988Z on 1989 April 5

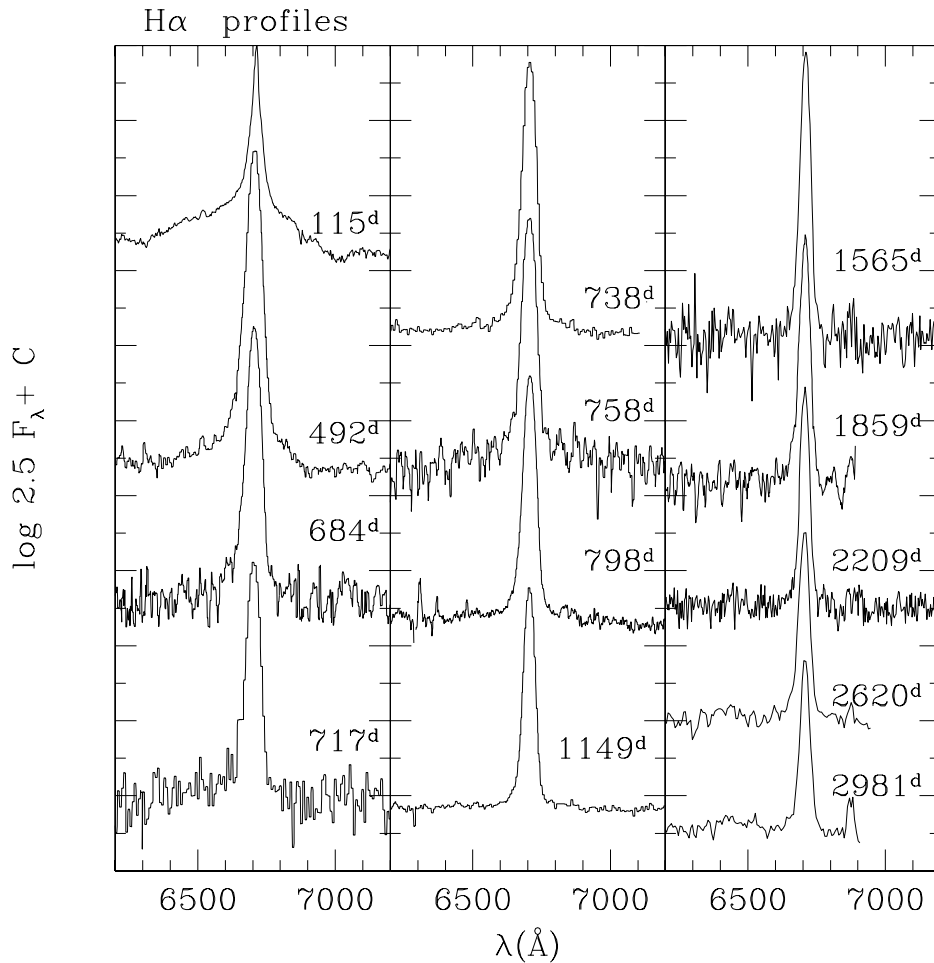


Figure 4. Evolution of H α profile

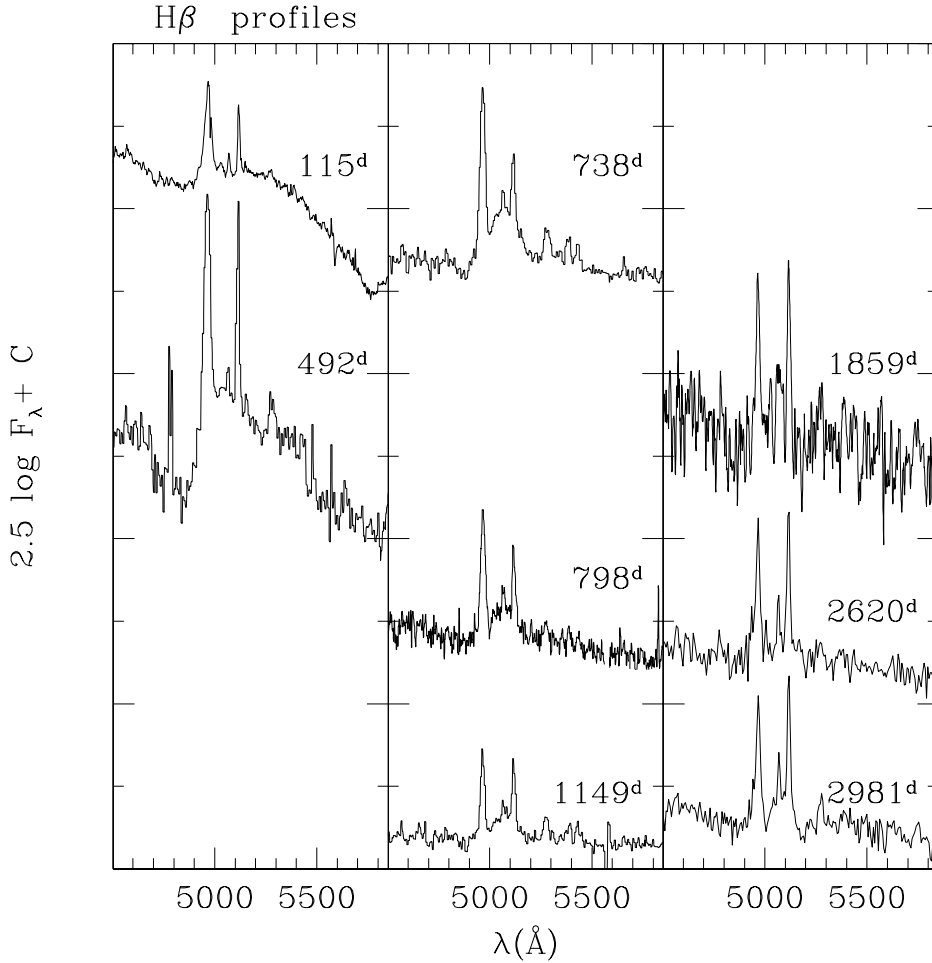


Figure 5. Evolution of H β profile

$$f_{\text{ion}} = q(\text{H}^0) h \overline{\nu}_{\text{ion}} \quad , \quad (2)$$

where $\overline{\nu}_{\text{ion}}$ is the mean frequency of the ionizing photons, approximately 27 eV. For case B recombination, the H α flux is related to the flux of ionizing photons by $f_{\text{H}\alpha} = 1.367088 \times 10^{-12} q(\text{H}^0)$ in c.g.s. units (Kennicutt 1988, Osterbrock 1989). Thus the conversion between the fluxes is

$$f_{\text{ion}} \approx 32 f_{\text{H}\alpha} \quad . \quad (3)$$

Figure 10 shows the SED at six stages in the evolution of SN 1988Z. Solid squares correspond to the flux values which were interpolated from those in table 4, and in the case of the ionizing continuum, estimated using equation 3. Open squares indicate that we have performed an extrapolation using the fits of Van Dyk et al. (1993) for radio wavelengths, or a $t^{-11/7}$ law drawn from the nearest value of optical points and from the H α or X-rays for the hard radiation. Therefore, open symbols should be taken with caution. The only exception being values extrapolated from data which are ± 50 days away, in which case these are represented as solid squares too. Crosses correspond to the H α line-free R_{cont} flux.

The SED of SN 1988Z differs from the SED of classical

SNe in that its high energy distribution is very prominent. There is also an indication that the shape in the early evolution differs from the general assumption that the emergent spectrum is created by an expanding hot atmosphere with mainly a Planckian output (e.g. Catchpole et al. 1989, Eastman & Kirshner 1989). The dashed line in Figure 10 shows what the SED would look like if the optical colours of SN 1988Z were to be interpreted as a blackbody distribution, as has been assumed in the case in other type II SNe (e.g. Wegner & Swanson 1996). Hard-radiation and radio excesses are expected when the SN shock interacts with a CSM. At this stage we are viewing the kinetical reprocessing of a SN remnant

4.2. Radiated energy estimates

In order to calculate the energy radiated by SN 1988Z in the first eight years of its evolution, first we integrate the light curves of Figure 2, interpolating linearly in the time-axis between the observed points, i.e. with no further extrapolation on the behavior of the light curves after the last observational point. This will give us an estimate of the observed

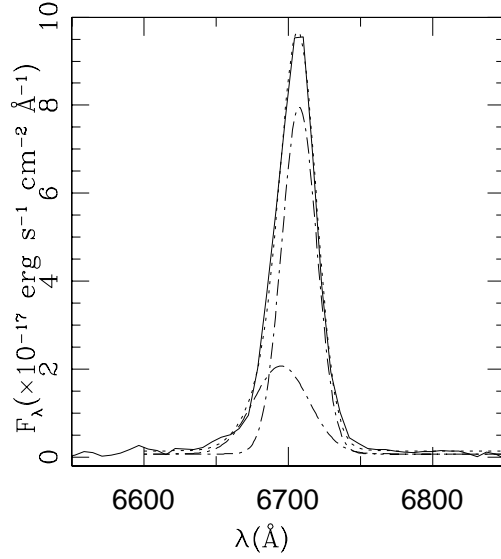


Figure 6. Multicomponent fit of the H α line of the spectrum taken on 1996 February 14. The parameters of the components are given in table 5. The dot-dashed lines represent single gaussian components, while the solid line and dotted line represent the spectrum and the fit.

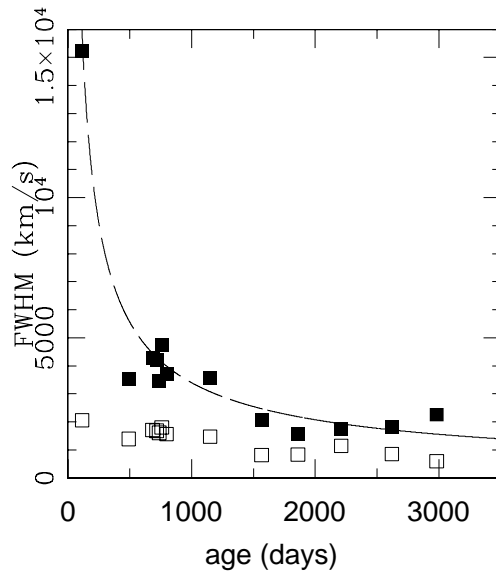


Figure 7. Evolution of the H α line profile. Solid squares represent the broad component and empty squares represent the intermediate component. The dashed line represents the law for the velocity shock evolution of a cSNR.

radiated energy during these eight years, which should be regarded as a lower limit to the total energy radiated during that time. Table 6 gathers the results, where time refers to the maximum span of the light curve in that band. From this table we derive that the observed emitted energy of SN 1988Z is dominated by the optical to X-ray radiation, having emitted at least 1.0×10^{51} erg in eight years.

This is a very rough estimate, which leaves gaps in the spectral energy distribution and in the time evolution at the

different bands. As an example, if we interpolate linearly the monochromatic flux at frequencies between B and V and V and R -bands along the evolution of the light curve, i.e.

$$E_{\text{opt}} = 4\pi d^2 \int_0^{8.2\text{yr}} dt \int_{\nu_R}^{\nu_B} d\nu f_\nu \quad , \quad (4)$$

where d is the distance to the cSNR, then we obtain that

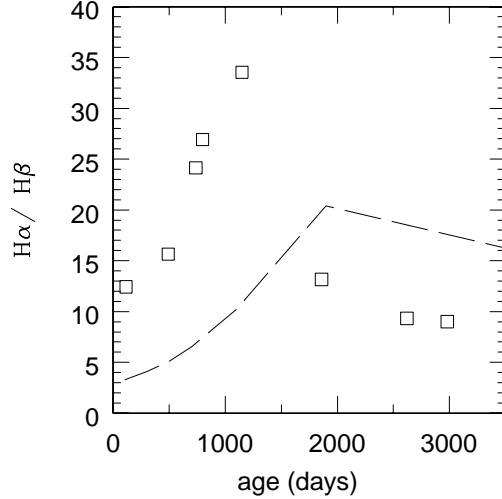


Figure 8. Evolution of the Balmer decrement (empty squares). The dashed line represents the theoretical values for the evolution of a cSNR.

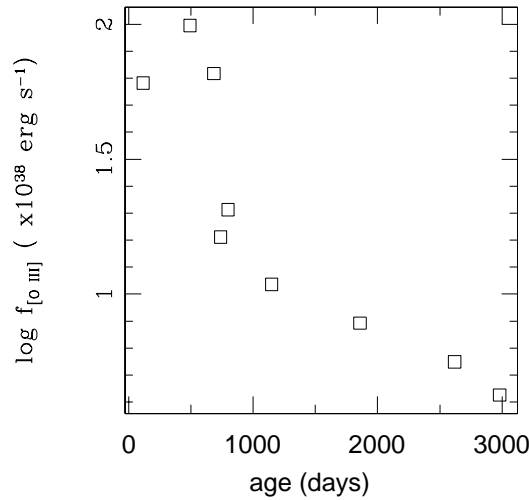


Figure 9. Evolution of [O III]λ5007 Å line

the energy radiated from B to R band is 1.6×10^{50} erg, or 1.5×10^{50} erg if using R_{cont} instead of R .

In order to obtain a more complete estimate of the emission at optical-UV wavelengths, we have performed an extrapolation of the B , V and R_{cont} fluxes to cover the 912Å to $1\mu\text{m}$ range, assuming that the SED is a power-law, i.e. $f_\nu \propto \nu^\alpha$, where α is calculated from the $B - V$ colours for the UV to V -band interval (typically $-3.0 < \alpha < -0.5$) and from the $V - R_{\text{cont}}$ colours for the V -band to $1\mu\text{m}$ interval (typically $-2 < \alpha < 5$). If the color doesn't change dramatically between these regions, the optical energy inferred is of the order of 3.2×10^{50} erg for the eight year evolution.

The ionization energy, in turn, can be estimated from the integration of the $H\alpha$ light curve. The use of eq. 3 gives a value of 8.7×10^{50} erg.

To estimate the radiation at 0.2–2 keV, we have extrapolated the three X-ray points to earlier epochs than 6.5 yr, when the first ROSAT observation was obtained. If we adopt

the $t^{-11/7}$ law before day 2355, so that at day 2355 it reproduces the first ROSAT observation, we have that the energy radiated in 3000 days in the 0.2–2 keV band could be as high as 6.0×10^{50} erg. If a complete bremsstrahlung spectrum of 1 keV is considered, the energy emitted in X-rays alone could be about 9.6×10^{50} erg, and if we consider internal absorption of the CSM, this could go up to 7.6×10^{51} .

These estimated values of the emitted energy in the 8.5 yr of evolution of SN 1988Z at different wavelengths are summarized in Table 7. Beware that some entries in this table are subsets of other entries (e.g. 4000–7000Å and 912– $1\mu\text{m}$), and that some entries are in part the result of reprocessing the energies of other entries (e.g. 912– $1\mu\text{m}$ and bremsstrahlung). Considering that half of the leading shock radiated energy is emitted outwards and the other half inwards and is therefore reprocessed by the high density thin shell, the total energy radiated in the event should include either twice the observed X-ray luminosity or the sum of

Table 6. Integrated values of observed emitted energy in different wavelengths

band	time yr	energy erg
0.2–2 keV	2.0	3.6×10^{48}
ionization	8.2	8.7×10^{50}
<i>B</i>	4.3	4.0×10^{49}
<i>V</i>	6.1	2.6×10^{49}
<i>R</i>	8.2	5.8×10^{49}
R_{cont}	8.2	3.7×10^{49}
2 cm	2.3	2.4×10^{46}
3.6 cm	2.4	2.2×10^{46}
6 cm	3.0	1.4×10^{46}
20 cm	2.3	1.4×10^{45}

Table 7. Integrated values of estimated emitted energy in different wavelengths during the 8.5 yr of evolution

band	energy erg
bremsstrahlung	9.6×10^{50} to 7.6×10^{51}
0.2–2 keV	6.0×10^{50} to 4.8×10^{51}
ionization	8.7×10^{50}
4000–7000Å	1.5×10^{50}
912Å– $1\mu\text{m}$	3.2×10^{50}

the observed X-ray luminosity and the inferred ionizing and optical luminosity, or twice the sum of the observed ionizing and optical luminosity.

A strong lower limit of the total radiated energy is then $2 \times 8.7 \times 10^{50} + 3.2 \times 10^{50} \approx 2 \times 10^{51}$ erg. The bolometric light curve derived for this estimate is represented with a thick solid line in figure 2.

A best estimate of the total radiated energy requires a model-dependent extrapolation either from the X-ray or from the $\text{H}\alpha$ radiation. The X-ray derived values are rather uncertain, since they require the assumption of time, spectral and absorption corrections. Allowing for these uncertainties, the energy could be as high as $2 \times 7.6 \times 10^{51} \approx 10^{52}$ erg. The bolometric light curve derived for this model-dependent estimate is represented with a thick dashed line in figure 2. Note that the excess energy of this second estimate is produced mainly at early epochs. A high value of the X-ray radiated energy is supported by the ionization energy estimates. The models indicate that during the earlier stages of evolution the emitted radiation is very hard and most of it leaves the remnant without producing ionization. A rough estimate based on the simple model indicates that the total energy radiated is about six times larger than the ionizing radiation, that is about 4×10^{51} . Recalling that this includes only half of the total energy emitted, we conclude again that the total energy radiated may be close to 10^{52} .

We emphasize that these estimates totally disregard any intrinsic reddening produced in the host galaxy or in the CSM of SN 1988Z.

5. DISCUSSION

We have shown that the integrated light emitted in radio, optical and X-rays by SN 1988Z in the 8.5 yr of evolution after discovery is of the order of several times 10^{51} erg and may be close to 10^{52} erg, i.e. larger than the canonical value of the kinetic energy released in a SN explosion, while typical SNe radiate one to two orders of magnitude less energy (e.g. Panagia et al. 1980, Catchpole et al. 1987, 1989). The value of the radiated energy in SN 1988Z is slightly smaller than that estimated for the most energetic kinetical release in a SN explosion observed so far, $(2 - 5) \times 10^{52}$ erg, in SN 1998bw (Galama et al. 1998, Iwamoto et al. 1998). Indeed on the basis of our result we speculate that SN 1988Z was a hypernova and may have been caused by the formation of a black hole in the core of a massive star. Most of the energy in SN 1988Z is radiated in the optical to X-ray interval, with spectra, SED and light curves departing from those of classical SN II. The high densities derived from the O forbidden lines and the flat light-curves strongly support the idea of a high-density circumstellar shell reprocessing the kinetic energy through fast radiative shocks.

The estimated CSM mass swept by the shock in this time is of the order of $15M_{\odot}$ (eq. A8), although this quantity is dependent on the assumed model. Chugai & Danziger (1994), for example, give an estimate of only about $1M_{\odot}$ from their own models.

While a detailed comparison of light-curve, SED, and line profile evolution is still missing, we have shown that the simplified model of ejecta interacting with a dense and homogeneous CSM outlined in the appendix reproduces the overall decay of the optical light, the level of X-ray and $\text{H}\alpha$ emission and its line-width evolution. The evolution of the $\text{H}\alpha$ flux is however more rapid than that predicted by the canonical models, and the absolute values of line-widths and Balmer decrements differ sometimes by more than a factor of 2. More fine-tuned models, possibly introducing a small density gradient in the circumstellar shell, are thus required.

Observationally much work is also needed, on one hand to identify cSNR like SN 1988Z early enough in their evolution, and on the other to obtain good quality data over the widest possible spectral range and time coverage. High-quality and high-resolution spectral information is particularly needed in the X-ray region early enough in the evolution of the SN, where and when most of the energy is radiated. A close optical monitoring of these objects would allow us to assess the predicted existence of modulations in the light curve decay and line component anomalies in the spectra due to catastrophic radiative cooling, and the precise dating of the disappearance of the broad emission lines.

ACKNOWLEDGMENTS

We would like to thank G. Tenorio-Tagle for useful suggestions on an early version of this paper. This work has been supported in part by the ‘Formation and Evolution of Galaxies’ network set up by the European Commission under contract ERB FMRX-CT96-086 of its TMR programme.

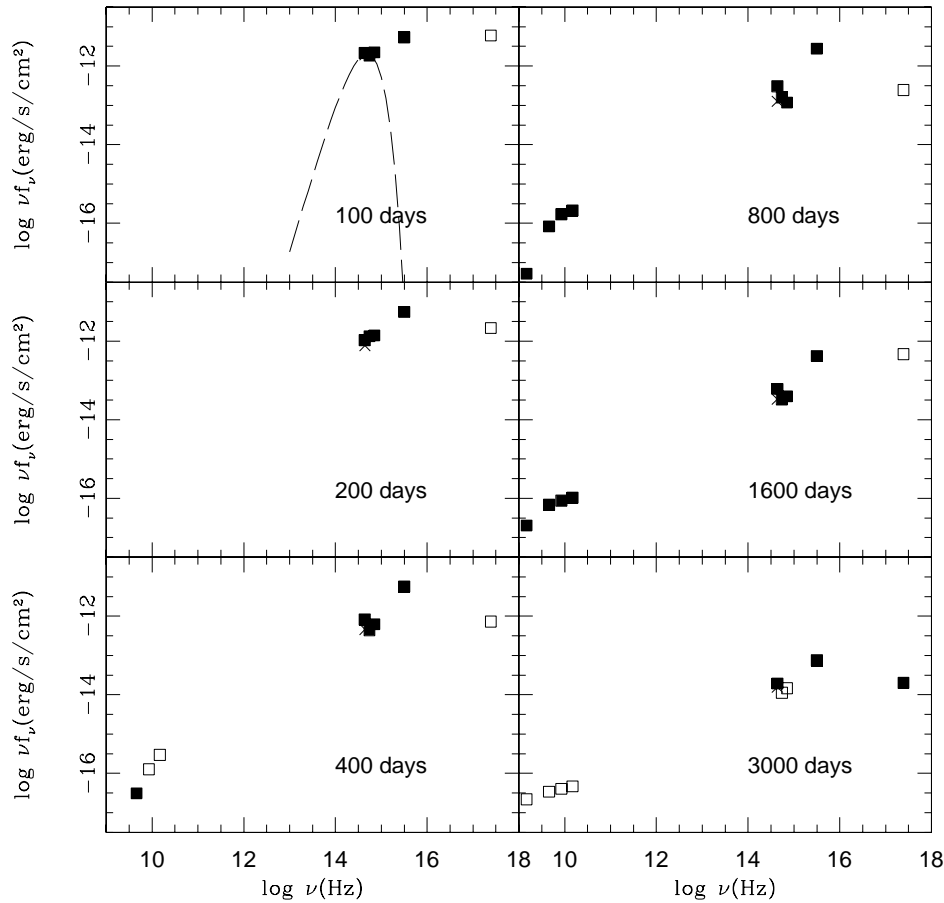


Figure 10. SED evolution of SN 1988Z: solid squares correspond to interpolations from values actually observed, and empty squares correspond to extrapolations. Crosses correspond to the $H\alpha$ line-free R_{cont} flux. The dashed line represents a blackbody at 5800 K.

REFERENCES

- Avedisova, V. S., 1974, *Sov Astr.*, 18, 283
 Barbon R., Cappellaro E. & Turatto M., 1989, *AAS*, 81,421
 Barbon R., Ciatti F. & Rosino L., 1979, *AA*, 72,287
 Bertschinger E., 1986, *ApJ*, 304, 154
 Bregman J.N., Pildis R.A., 1992, *ApJ*, 398,107
 Burstein D. & Heiles C., 1982, *AJ*, 87,1165
 Cappellaro E. & Turatto M. 1988, *IAU Circ.* 4691
 Catchpole et al., 1987, *MNRAS*, 229,15P
 Catchpole et al., 1989, *MNRAS*, 237,55P
 Chevalier R. A., and Imamura J. N., 1982, *ApJ*, 261, 543
 Chevalier R. A., 1974, *ApJ*, 188, 501
 Chugai N.N., 1991, *MNRAS*, 250,513
 Chugai N.N. & Danziger, 1994, *MNRAS*, 268,173
 Cioffi D. F., McKee C. F., and Bertschinger, E., 1988, *ApJ*, 334, 252
 Draine B.T. and Woods D.T., 1991, *ApJ*, 383, 621
 Eastman R.G. & Kirshner R.P., 1989, *ApJ*, 347,777
 Fabian A.C., Terlevich R.J., 1996, *MNRAS*, 280,L5
 Falle S. A. E. G., 1975, *MNRAS*, 172,55
 Falle S. A. E. G., 1981, *MNRAS*, 95, 1011
 Ferland G.J., 1997, *Hazy, a brief introduction to CLOUDY 90'*, Univ. of Kentucky at Lexington.
 Filippenko, A.V., 1997, *ARAA*, 35,309
 Filippenko A.V. 1991, in 'Supernovae', Ed. S.E. Woosley, Springer-Verlag, page 467.
 Filippenko A.V., 1989, *AJ*, 97,726
 Galama T.J. et al., 1998, *Nat*, 395,67
 Gaskell C.M., Koratkar A.P., 1989, *IAU Circ.* 4761
 Hamuy M., Suntzeff N.B., Heathcote S.R., Walker A.R., Gigoux P., Phillips M.M., 1994, *PASP*, 106,566
 Imamura J. N., 1985, *ApJ*, 296, 128
 Iwamoto K. et al., 1998, *Nat*, 395, 672.
 Kennicutt R.C., 1988, *ApJ*, 334, 144
 Landolt A.U., 1992, *AJ*, 104,340
 McCray R, Stein R. F., and Kafatos M., 1975, *ApJ*, 196, 565
 Osterbrock D.E. 1989, "Astrophysics of Gaseous Nebulae and Active Galactic Nuclei", University Science Books.
 Panagia N. et al. 1980, *MNRAS*, 192, 861.
 Plewa T., 1995, *MNRAS*, 275, 143.
 Pollas C., 1988a, *IAU Circ.* 4691
 Pollas C., 1988b, *IAU Circ.* 4696
 Pollas C., 1989, *IAU Circ.* 4742
 Salamanca I., Cid Fernandes R., Tenorio-Tagle G., Telles E., Terlevich R.J., Muñoz-Tuñon C., 1998, *MNRAS*, 300,L17
 Schlegel E.M., 1990, *MNRAS*, 244,269
 Seaton M.J., 1979, *MNRAS*, 187,73P
 Shull J.M., 1980, *ApJ*, 237,769
 Stathakis R.A., Sadler E.M., 1991, *MNRAS*, 250,786
 Tenorio-Tagle G., Bodenheimer P., Franco J., and Rozyczka M., 1990, *MNRAS*, 244, 563
 Terlevich R.J., 1994, in Clegg R.E.S., Stevens I.R., Meikle W.P.S.,

eds, Circumstellar Media in the Late Stages of Stellar Evolution. Cambridge Univ. Press, Cambridge, p. 153

Terlevich R.J., Tenorio-Tagle G., Franco J., Melnick J., 1992, MNRAS, 255,713

Turatto M., Benetti S., Cappellaro E., Danziger I.J., Mazali P.A., 1999, in 'SN 1987A: Ten Years After', eds. M.M. Phillips, N.B. Suntzeff, Fifth CTIO/ESO/LCO Workshop, in press.

Turatto M., Cappellaro E., Danziger I.J., Benetti S., Gouiffes C., Della Valle M., 1993a, MNRAS, 262,128

Turatto M., Cappellaro E., Benetti S., Danziger I.J., 1993b, MNRAS, 265, 471.

Van Dyk S.D., Weiler K.W., Sramek R.A., Panagia N., 1993, ApJL, 419,L69

Wegner G. & Swanson S.R., 1996, MNRAS, 278, 22.

Wheeler J.C., Mazurek T.J. & Sivaramakrishnan, 1980, ApJ, 237,78

APPENDIX A: THE “SIMPLE MODEL” FOR COMPACT SUPERNOVA REMNANTS

The interaction of the SN ejecta with a dense CSM causes a shocked region of hot gas enclosed by two shock waves: on the outside the leading shock, and on the inside the inward facing “reverse” shock. The leading shock ($v_s \sim 10^4 \text{ km s}^{-1}$) encounters dense circumstellar material and raises its temperature to $\sim 10^9 \text{ K}$. The reverse shock, which is initially substantially slower ($v \sim 10^3 \text{ km s}^{-1}$), begins to thermalize the supernova ejecta to temperatures of about 10^7 K . Early analytical and numerical computations of the evolution of SNRs in a dense medium (Chevalier 1974; Shull 1980; Wheeler et al. 1980) showed a speeded-up evolution compared with the “standard” solution in a medium of $n_0 = 1 \text{ cm}^{-3}$. All evolutionary phases (free expansion, thermalization of the ejecta, the quasi-adiabatic Sedov phase, the radiative and the pressure modified snow-plough phases) which have been thoroughly studied for the standard case, are substantially speeded up as a consequence.

Supernova remnants evolving in a dense CSM reach their maximum luminosity ($L > 10^8 L_\odot$) at small radii ($R < 0.1 \text{ pc}$) soon after the SN explosion ($t < 20 \text{ yr}$) while still expanding at velocities of more than 1000 km s^{-1} (Shull 1980; Wheeler et al. 1980; Draine and Woods 1991; Terlevich et al. 1992; Terlevich 1994). In these cSNR, radiative cooling becomes important well before the thermalization of the ejecta is complete. As a result, the Sedov phase is avoided and the remnant goes directly from the free expansion phase to the radiative phase. The shocked matter undergoes a rapid condensation behind both the leading and the reverse shocks. As a consequence two high-density, fast-moving thin shells are formed. These dense shells, the freely expanding ejecta and a section of the still dynamically unperturbed interstellar gas, are all ionized by the radiation from the shocks.

For SNe evolving in CSM densities of the order of $n_0 \sim 10^7 \text{ cm}^{-3}$, the cooling-time (t_c) and cooling-length (r_c) scales for the post-shock temperatures are very small.

$$t_c \simeq \frac{3kT_s}{8n_0\Lambda} \simeq 0.2 \frac{v_8^2}{n_7\Lambda_{23}} \text{ yr}, \quad (\text{A1})$$

$$r_c \simeq \frac{1}{4} t_c v_s \simeq 1.8 \times 10^{14} \frac{v_8^3}{n_7\Lambda_{23}} \text{ cm}, \quad (\text{A2})$$

where v_8 is the velocity in 10^8 km s^{-1} units, n_7 is the density

in 10^7 cm^{-3} units, Λ_{23} is the cooling function (Λ) in $10^{-23} \text{ erg cm}^3 \text{ s}^{-1}$ units, T_s is the shock temperature, and k is Boltzmann’s constant. Thus, radiative losses become important at very early times when the shock velocities and temperatures are $v_s > 10^3 \text{ km s}^{-1}$ and $T_s > 10^7 \text{ K}$, well before the ejecta is even thermalized. This means that a large flux of ionizing photons will emerge from the shocked gas at X-ray energies.

For a supernova remnant which injects 10^{51} ergs into a medium of constant density n_7 , the onset of the radiative phase behind the leading shock which causes the formation of a dense outer shell, assuming free-free cooling only, (Shull 1980, Wheeler et al. 1980, Draine and Woods 1991) begins at a time t_{sg} , given by

$$t_{sg} = 230 E_{51}^{1/8} n_7^{-3/4} \text{ days} \quad (\text{A3})$$

where E_{51} is the energy deposited by the SN in units of 10^{51} ergs. At this stage, the shock is at a radius

$$R_s = 0.01 E_{51}^{1/4} n_7^{-1/2} \left(\frac{t}{t_{sg}} \right)^{2/7} \text{ pc}, \quad (\text{A4})$$

with velocity

$$v_s = 4600 E_{51}^{1/8} n_7^{1/4} \left(\frac{t}{t_{sg}} \right)^{-5/7} \text{ km s}^{-1}, \quad (\text{A5})$$

temperature

$$T_s = 3.0 \times 10^8 E_{51}^{1/4} n_7^{1/2} \left(\frac{t}{t_{sg}} \right)^{-10/7} \text{ K}, \quad (\text{A6})$$

and luminosity

$$L_s = 2 \times 10^{43} E_{51}^{7/8} n_7^{3/4} \left(\frac{t}{t_{sg}} \right)^{-11/7} \text{ erg s}^{-1}. \quad (\text{A7})$$

The mass swept by the shock is

$$M_{shell} = 1.1 E_{51}^{3/4} n_7^{-1/2} \left(\frac{t}{t_{sg}} \right)^{6/7} M_\odot. \quad (\text{A8})$$

These approximate formulae assume that the ejecta has already been fully thermalized. However, for the case of interest in this work (i.e. for $n_0 \geq 10^5 \text{ cm}^{-3}$) strong radiative losses occur before thermalization is complete. Because the cooling processes radiate the thermal energy at the same rate as thermalization proceeds, the Sedov phase is totally inhibited and thus there is no self-consistent analytic treatment for the evolution of such remnants. It is therefore necessary to follow the detailed time evolution of the gas flow. In particular, special care should be given to the post-shock structure which is sensitive to the details of the ambient density distribution and to the temperature dependence of the radiative cooling function.

The cooling time scale, t_c , for an optically thin plasma, is proportional to the inverse of the gas density and the evolution proceeds faster at higher ambient densities. On the other hand, the temperature dependence of the cooling function is different for different temperature ranges. Adiabatic shocks are stable but cooling instabilities can develop over a wide range of radiative shock conditions (Avedisova 1974, Falle 1975, 1981, McCray, Stein and Kafatos 1975, Chevalier and Imamura 1982, Imamura 1985, Bertschinger 1986).

The details of the transition from a nearly adiabatic to a strongly radiative shock depend on the ability of the gas to readjust to the cooling rate. Pressure gradients tend to

be smoothed out in a sound-crossing time, t_d , and the ratio t_c/t_d provides an estimate of the conditions prevailing in the cooling gas. For $t_c/t_d > 1$, at moderate cooling rates, the gas elements are continuously compressed as their temperature falls and the cooling process operates quasi-isobarically at the pressure attained by the gas immediately behind the shock. For $t_c/t_d < 1$, however, the cooling rate dominates over any pressure readjustment and the process becomes quasi-isochoric at the post-shocked density of the cooling gas elements.

A large pressure imbalance then develops in the flow, and new additional shocks are generated which end up compressing the cooled gas. This process, termed “catastrophic cooling” (Falle 1975, 1981), appears during thin shell formation and the instabilities continue to operate during the rest of the radiative shock evolution (Chevalier and Imamura 1982; Bertschinger 1986; Cioffi, McKee & Bertschinger 1988; Tenorio-Tagle et al 1990). The catastrophic cooling acquires a central role in the case of supernovae evolving in high density media due to the strength of the radiation produced upon cooling, and the rapid variations inherent in the shock propagation. These features imply that a large flux of ionizing photons will emerge from the shocked gas. The wide range of gas temperatures in the cooling region results in a power-law-like spectrum at UV and X-ray frequencies (Terlevich et al. 1992).